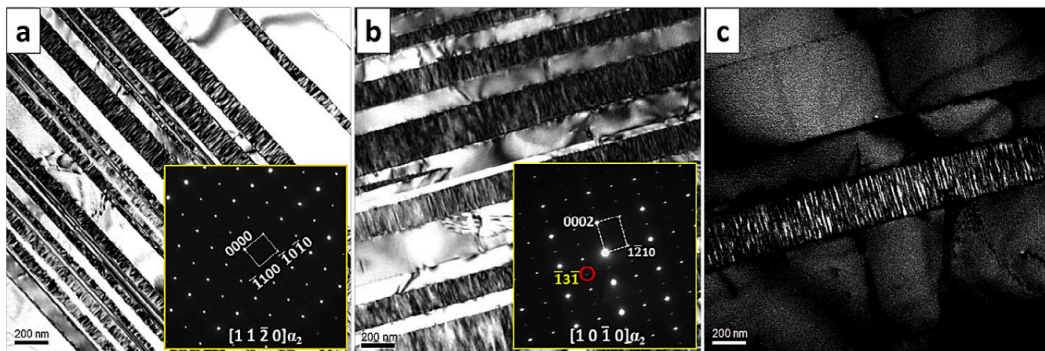


**Fig. 2.** Bright-field TEM micrographs of modulated  $\alpha_2$  laths with SAED pattern along  $\langle 11\bar{2}0 \rangle \alpha_2$  (a), along  $\langle 10\bar{1}0 \rangle \alpha_2$  (b), and dark-field micrograph recorded by a reflection of the O phase indicated by a circle (c).

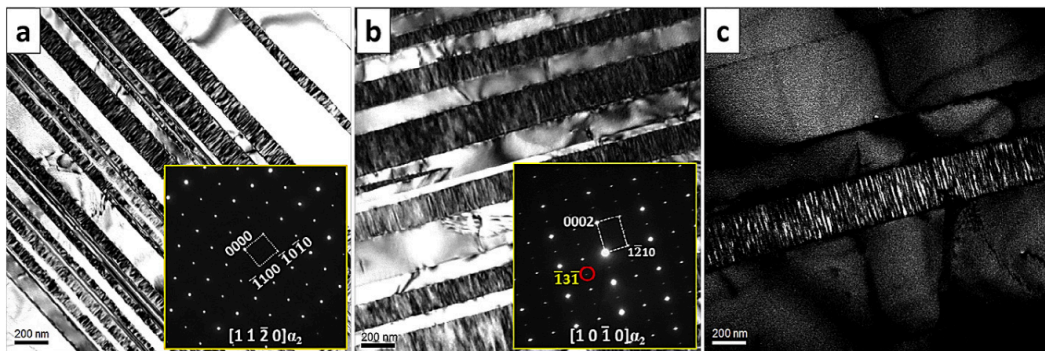
The microstructure of the  $\gamma$ -based Ti-45Al-8.5Nb alloy observed by SEM in BSE mode is a near fully-lamellar microstructure with an average grain size of 62  $\mu\text{m}$ , as shown in Fig. 1. Lamellar colonies composed of alternating  $\alpha_2+\gamma$  laths are arranged randomly. The bright contrast phases often located at the peripheries of the lamellar colonies are the remnant B2 phase [21,22], and the volume fraction of remnant B2 phases was estimated to be about 5%.

Fig. 2(a and b) are bright-field TEM micrographs of the microstructure slightly off the  $\langle 11\bar{2}0 \rangle \alpha_2$  and  $\langle 10\bar{1}0 \rangle \alpha_2$  directions, respectively, showing a nano-scale modulated structure with tweed contrast within  $\alpha_2$  laths on the  $\gamma/\alpha_2$  lamellae edge-on projection. The chemical composition analyses were carried out for the  $\gamma$  phase and modulated  $\alpha_2$  laths (ML) in the alloy by EDS, and the results are shown in Table 1. The SAED pattern of the modulated structure along  $\langle 11\bar{2}0 \rangle \alpha_2$  is inserted in Fig. 2(a), which shows no additional reflections besides those of the  $\alpha_2$  phase. The SAED pattern of the modulated structure along  $\langle 10\bar{1}0 \rangle \alpha_2$  is inserted in Fig. 2(b), in which the reflections at positions along the  $\langle 0001 \rangle \alpha_2$  direction extinct for the  $\alpha_2$  phase were observed. These reflections can be indexed as those in the pattern of  $\langle 310 \rangle_0$  of the O phase, according to orientation relationships of  $\langle 001 \rangle_0 // \langle 0001 \rangle \alpha_2$  and  $\langle 100 \rangle_0 // \langle 11\bar{2}0 \rangle \alpha_2$  reported in the literature [2]. A dark-field TEM micrograph recorded from a reflection of the O phase is shown in

Fig. 2(c), indicating a needle-like morphology of the O phase at nano-scale within  $\alpha_2$  laths. The needles of the O phase are vertical to the  $\alpha_2/\gamma$  interface with  $\langle 0001 \rangle \alpha_2 // \langle 111 \rangle \gamma$ . One can find that the most of the O phase needles form at the  $\alpha_2/\gamma$  interface and terminate inside the  $\alpha_2$  lath. It is speculated that a mismatch between  $\alpha_2$  and  $\gamma$  phases favors heterogeneous nucleation of the O phase at the  $\alpha_2/\gamma$  interface.



**Fig. 2.** Bright-field TEM micrographs of modulated  $\alpha_2$  laths with SAED pattern along  $\langle 11\bar{2}0 \rangle \alpha_2$  (a), along  $\langle 10\bar{1}0 \rangle \alpha_2$  (b), and dark-field micrograph recorded by a reflection of the O phase indicated by a circle (c).



**Fig. 2.** Bright-field TEM micrographs of modulated  $\alpha_2$  laths with SAED pattern along  $\langle 11\bar{2}0 \rangle \alpha_2$  (a), along  $\langle 10\bar{1}0 \rangle \alpha_2$  (b), and dark-field micrograph recorded by a reflection of the O phase indicated by a circle (c).

# EPFL Example TEM data analysis